

PAPER • OPEN ACCESS

## Synthesis, characterization and application of analcime to control nitrate ions from the ground water samples from Wadi El-Assiuti – Egypt as a low-cost and locally available adsorbent

To cite this article: Ahmed A. Abdelmoneim *et al* 2020 *IOP Conf. Ser.: Mater. Sci. Eng.* **975** 012013

View the [article online](#) for updates and enhancements.

You may also like

- [Design and Fabrication of a Highly Stable Polymer Carbon Nanotube Nanocomposite Chemiresistive Sensor for Nitrate Ion Detection in Water](#)  
Ashwini N. Mallya and Praveen C. Ramamurthy
- [The oscillation of an infinite plate in a strong rarefied gas under constant force](#)  
M A Abdel-Gaid, M A Khidr and A E El Safty
- [Bulk- and electrode-limited conduction mechanisms in different phases of Mn<sup>2+</sup>-doped potassium tetrachlorozincate crystal](#)  
M A Gaffar, A M Abousehly, A Abu El-Fadl *et al.*



**245th ECS Meeting**  
San Francisco, CA  
May 26–30, 2024

**PRiME 2024**  
Honolulu, Hawaii  
October 6–11, 2024

Bringing together industry, researchers, and government across 50 symposia in electrochemistry and solid state science and technology

Learn more about ECS Meetings at  
<http://www.electrochem.org/upcoming-meetings>

 Save the Dates for future ECS Meetings!

# Synthesis, characterization and application of analcime to control nitrate ions from the ground water samples from Wadi El-Assiuti – Egypt as a low-cost and locally available adsorbent

**Ahmed A. Abdelmoneim<sup>1</sup>, Mohamed Abdul-Moneim<sup>2</sup>, Ahmed A Geies<sup>3</sup>, and Seham O. Farghaly<sup>1</sup>**

<sup>1</sup>Geology Departments, Faculty of Science, Sohag University, Sohag, Egypt.

<sup>2</sup>Geology Department, <sup>3</sup>Chemistry Department, Faculty of Science, Assiut University, Assiut, Egypt.

**Abstract.** In this study, the sorption behavior of synthetic (Analcime) zeolites with respect to nitrate ions has been studied in order to consider its application to purity ground water. Analcime or also can be called analcite (“weak”) is a kind of grey, white or colorless tectosilicates minerals. It is hydrated sodium aluminum silicates which exist in cubic form in crystalline. Analcime was successively synthesized from kaolinite as a raw material using the fusion with NaOH method. The conditions of hydrothermal crystallization (zeolitization) were found to be at temperature of 170 C°, and time span between 36 h and 72 h for kaolinite with the molar composition of 6Na<sub>2</sub>O: 0.75Al<sub>2</sub>O<sub>3</sub>:30SiO<sub>2</sub>. 780H<sub>2</sub>O. The synthetic materials have been characterized by X-ray diffraction (XRD), scanning electron microscope (SEM), Fourier transform infrared spectroscopy (FT-IR), thermo gravimetric (DTA/TGA) analysis and Surface area and porosity of synthesized analcime. The results indicate that the crystallization of analcime not affected by the hydrothermal reaction time. Also analcime was tested as adsorbents for the removal of nitrate ions from the ground water samples from Wadi El-Assiuti – Egypt. The adsorption capacities of nitrate ions by analcime, as a function of its concentration, were determined at room temperature by varying analcime concentration for each water samples. During the process, all the other parameters (pH and contact time) were kept constant with respect to the initial concentration of nitrate ions in the water samples. It was found analcime has good removal efficiency obtained at pH 6-7.6, adsorbent dosage 10-12 g/L, and contact time 60 min. The Langmuir constants model for NO<sub>3</sub><sup>-</sup> ion sorption on the adsorption isotherms is fitted well. The R<sub>L</sub> value in the present investigation was equal or less than one, indicating that the adsorption of NO<sub>3</sub><sup>-</sup> ion by analcime is favorable.

**Keywords.** Analcime, Ground water, Characterization, Element contents, Water treatment.

## 1. Introduction

Groundwater begins with precipitation that seep into the ground. It refers to the water that is stored in the pervious, porous and permeable rocks referred to as aquifers, everywhere in the world. Depending on the rock type and formation, groundwater is found in the ground within the depth of 100 meters and in some places up to 1000 meters deep. A great percentage of people worldwide use this source of water for their agricultural, domestic and industrial purposes [1]. Variation in groundwater chemistry is mainly a function of the interaction between the groundwater and the mineral composition of the aquifer materials through which it moves. Hydro-chemical processes, including dissolution, precipitation, ion exchange, sorption, and desorption, together with the residence time occurring along the flow path, control the variation in chemical composition of groundwater [2]. Nitrate, due to its high water solubility, is possibly the most widespread groundwater contaminant in the world, seriously threatening supplies of drinking water and promoting eutrophication [3]. A high concentration of nitrate in drinking water leads to production of nitrosamine, which is related to cancer and increases the risk of diseases such as methemoglobinemia in newborn infants [4-6]. Hence,



reduction of nitrates in drinking water to permissible levels is mandatory. For these reasons, the US Environmental Protection Agency (EPA) and the World Health Organization (WHO) have defined a maximum contamination level (MCL) of 10 mg N-NO<sub>3</sub>-L in water. [7-8]. Various technologies have been used to remove nitrate from groundwater, including reverse osmosis, ultrafiltration, ion exchange, ion-exchange-membrane bioreactors, catalytic reduction, electro-dialysis, activated carbon, land disposal, chemical de-nitrification, and microbiological treatment [3], [9-10]. Zeolites are crystalline hydrated aluminum silicates with a framework structure containing pores that are occupied by water and by alkali and alkaline earth cations. Due to their high cation-exchange ability as well as molecular sieve properties, natural zeolites (cheap materials, easily available in large quantities in many parts of the world) show special importance in water and gas purification, adsorption and catalysis [11]. Zeolites have also an advantage over filter materials with significant permeability and are widely used for water purification by filtration [12-13]. Low-silica zeolites (LSZs) with Al/Si ratio of 1:1 are relatively rare [14]. These zeolites exhibit the highest ion exchange capacity and have important industrial applications. They are used as adsorbents or substitute for conventional phosphatic builder. Analcime is a hydrated sodium aluminum silicate which exists in cubic crystals. The chemical formula of analcime is NaAlSi<sub>2</sub>O<sub>6</sub>·H<sub>2</sub>O [15]. with small amount of potassium and calcium. The structure and chemical properties are more similar to the feldspathoids, even though they are classified to the zeolite mineral. Natural analcime can be found in the analcime basalt and other alkaline igneous rocks. Analcime can be used as an ion-sieve [16]. One of the analcime characteristics is exchange ions at room temperature, and increasing temperature make the ion-exchange more easily. This is due to the presence of smaller pores in analcime structure [17]. Generally, zeolite minerals are rare in the entire world, therefore over 200 synthetic zeolites have been synthesized either using chemicals or natural materials. In our study, it is aimed to purify nitrate ions from ground water by adsorption on synthesized analcime and to investigate the kinetics and equilibrium parameters involved during this adsorption. The parameters in this study included initial concentration, contact time, temperature, adsorbent dosage and influence of pH. Moreover, our work is to investigate the features of nitrates ion sorption from ground water by using synthetic zeolite analcime under static and dynamic conditions.

## 2. Hydrogeological setting of Wadi Assiuti

Wadi EL-Assiuti area represents a segment of the Nile valley in Upper Egypt. It is located on the fringes of the flood plane east of Assiut city. The area is bounded by latitudes 27° 5' N and 27°20' N and longitudes 31° 10'E and 31° 25'E. The area is located in an arid region with almost no rainfall. Temperature varies from 5 C° in winter to 45°C in summer. El fatah district is a part of Wadi EL-Assiuti area in Assiut governorate from its eastern side figure 1a, b. Several studies were previously carried out on this study area for dealing with its evaluation of its ground water potentiality. The study area is a rectangular flat area of about 400 Km<sup>2</sup>. It is bounded from the west by the Nile River and from the other sides by the limestone plateau that is dissected by a great number of wadis. Groundwater in this aquifer is characterized by fresh water. The salinity from 800 to 1000 mg/L. The salt assemblages are: Ca (HCO<sub>3</sub>)<sub>2</sub>, Mg (HCO<sub>3</sub>), NaHCO<sub>3</sub>, Na<sub>2</sub>SO<sub>4</sub> and NaCl which indicate a clear resemblance to the salt assemblages of surface water. The study of hydro-chemical characteristics in Wadi EL-Assiuti revealed on the high concentration of nitrate in some studied wells relative to [7-8].

## 3. Materials and Methods

Thirteen groundwater samples were collected from Wadi EL-Assiuti, for physical and chemical analyses. The samples were collected in clean polyester bottles which were thoroughly rinsed with sample water and tightly sealed and labeled after collection. These samples were kept in refrigerated and transferred to the laboratory for analysis.

All analyses were carried out in the geochemical laboratory of geology department, Faculty of Sciences, Sohag and Assiut University. The average of the analyses results are given in table 1a,b. Analcime was prepared by two methods using kaolinite raw materials as a source of Al and Si and

NaOH (Merck, Darmstadt, Germany) were used for zeolite synthesis. The various characteristics of the synthesized analcime were also identified include The X-ray diffractograms of analcime was obtained with a Philips X-ray unit (Phillips generator PW-1710) and Ni-Filtered  $\text{CuK}\alpha$  radiations. The morphology of analcime was examined by scanning electronic microscopy (SEM) using a Jeol JSM-5400 LV-ESM.

The FTIR spectra of the synthesized analcime that were obtained on a Shimadzu 2110 PC Scanning meter within the limits of 4,000–500  $\text{cm}^{-1}$  with a resolution of 0.5  $\text{cm}^{-1}$  (KBr pellets, CAN/KBr = 1/3 by mass, 6 atm.). (TGA) and differential thermal gravimetric (DTG) were carried out in air with Shimadzu DTG-60 at heating rate of 10°C/min. The chemical composition of the raw materials kaolinite are given in table 2.

**Table 1.a.** Results of the physical and chemical analyses of groundwater samples from Wadi EL-Assiuti

Well No	Units	pH	TDS ppm	Error %	EC $\mu\text{s}/\text{cm}$	Heavy metals			
						$\text{Fe}^{+2}$	$\text{Mn}^{+2}$	$\text{Cd}^{+2}$	$\text{Pb}^{+2}$
1	ppm	8.1	6003	2.7	9380	0.2	0.07	0.1	Nil
	eppm								
2	ppm	8.8	1536	-3.2	2400	Nil	0.05	Nil	Nil
	eppm								
3	ppm	8.8	198.4	2.5	310	Nil	Nil	Nil	Nil
	eppm								
4	ppm	8.3	3168	2.8	4950	0.14	Nil	Nil	Nil
	eppm								
5	ppm	9.1	198.4	1.6	310	Nil	Nil	Nil	Nil
	eppm								
6	ppm	8.1	4480	2.5	7000	0.16	Nil	Nil	Nil
	eppm								
7	ppm	8.2	1633	-2.4	2530	Nil	Nil	Nil	Nil
	eppm								
8	ppm	8.5	198.4	-1	3100	0.09	Nil	Nil	Nil
	eppm								
9	ppm	9.2	217.6	-4	340	Nil	Nil	Nil	Nil
	eppm								
10	ppm	8	3955	-0.06	6180	0.3	Nil	Nil	Nil
	eppm								
11	ppm	8.8	1740	0.15	2720	0.1	Nil	Nil	Nil
	eppm								
12	ppm	8.3	2112	-0.6	3300	0.2	Nil	Nil	0.2
	eppm								
13	ppm	8.4	198.4	1.4	3100	0.1	Nil	Nil	0.08
	eppm								

**Table 1.b.** Results of the physical and chemical analyses of groundwater samples from Wadi EL-Assiuti

Well No	Units	Major Cations				TH	Major Anions			
		Ca <sup>2+</sup>	Mg <sup>2+</sup>	Na <sup>1+</sup>	K <sup>1+</sup>		HCO <sup>1-</sup> <sub>3</sub>	Cl <sup>1</sup>	SO <sup>2-</sup> <sub>4</sub>	NO <sup>1-</sup> <sub>3</sub>
1	ppm	72	180	1700	17.6	921	490	2680	165	42
	epm	3.6	15	74	0.5		4.8	76	3.4	0.7
2	ppm	40	5.7	475	8.8	123	159	680	165	17
	epm	2	0.47	21	0.2		2.6	19	3.4	0.3
3	ppm	23	4.6	28	5.6	76	51	45	14	28
	epm	1.2	0.4	1.2	0.1		0.8	1.3	0.3	0.5
4	ppm	70	61	990	11	426	145	1480	165	80
	epm	3.5	5	43	0.3		2.4	42	3.4	1.3
5	ppm	22	4.5	33	6.5	74	25	50	25	41
	epm	1.1	0.4	1.4	0.2		0.4	1.4	0.5	0.7
6	ppm	82	61	1520	2.2	456	148	2275	165	94
	epm	4.1	5	66	0.1		2.4	64	3.4	1.5
7	ppm	75	5.4	535	21	209	84	800	165	74
	epm	3.7	0.4	23	0.5		1.4	23	3.4	1.2
8	ppm	87	5.4	685	13	240	95	1025	165	100
	epm	4.3	0.4	30	0.3		1.3	29	3.4	1.6
9	ppm	32	4.12	32.4	7.3	97	34	46	18	100
	epm	1.6	0.3	1.4	0.2		0.5	1.3	0.4	1.6
10	ppm	72	5.8	1590	13	204	84	2370	165	92
	epm	3.6	0.4				1.4	67	3.4	1.5
11	ppm	64	5.2	69	0.3	181	72	1011	19	79
	epm	3.2	0.4	675	11.		1.2	29	0.4	1.3
12	ppm	64	5.2	28	0.3	181	72	1011	165	72
	epm	3.2	0.4	746	13		1.2	29	3.4	1.2
13	ppm	82	5.6	33	0.3	228	91.5	1075	165	21
	epm	4.1	0.5	721	12.6		1.5	30	3.4	0.4

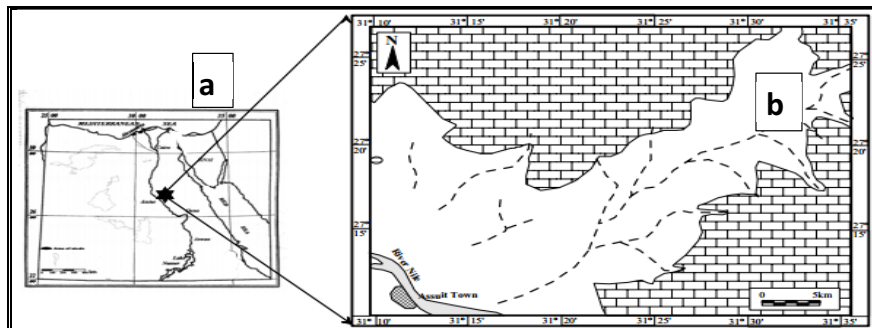


**Figure 1a, b.** Simplified geological and Location map of Wadi EL-Assiuti

**Table (2).**Chemical composition of kaolinite

Composition	SiO <sub>2</sub>	TiO <sub>2</sub>	Al <sub>2</sub> O <sub>3</sub>	Fe <sub>2</sub> O <sub>3</sub>	MnO	MgO	CaO	Na <sub>2</sub> O	K <sub>2</sub> O	P <sub>2</sub> O <sub>5</sub>	SO <sub>3</sub>
Content (wt. %)	49.2	2.82	32.97	6.82	0.24	2.2	9.43	0.8	0.05	0.13	0.26

### 3.1. Synthesis of analcime

By using alkaline fusion (after [18]) to synthetic analcime using kaolinite NaOH pellets was mixed with the calcinated Kaoline by ratio 1.2: 1 and the mixture was fused at 600 C° for 1 h . The alkaline reagent added to the starting material acts as an activator agent during fusion. The alkali-fused products were then dissolved in water (H<sub>2</sub>O/alkali fused starting material ratio )=(1:4.9), generally under stirring conditions until the reaction gels were homogenized aged for 24 h under static conditions. The mixtures were transferred into poly tetra fluoro-ethylene (PTFE) bottles of 200 ml and a stainless steel autoclave, then crystallized under static conditions at 170 C° for 5, 3, 1.5, days .After removal from the oven they were quenched in cold water and the product recovered by vacuum filtration, washed well with distilled water until the pH reach up to 11 and dried at 80 C° overnight.

Analcime was synthesized through a hydrothermal method using the following reaction condition: 6Na<sub>2</sub>O: 0.75Al<sub>2</sub>O<sub>3</sub>:30SiO<sub>2</sub>. 780H<sub>2</sub>O. At first, 4.75g of sodium hydroxide were dissolved in 10 g water. To this solution about 3.575 of kaolinite were added. The mixture was stirred (200-300 rpm), thereafter 161.25 g of water were added and stirred.

The gel was then transferred to poly tetra fluoro ethylene (PTFE) bottles (200 ml) and a stainless steel autoclave, and then put in oven at 170 C° for 36h.After removal from the oven, quenched in cold water, and the product recovered by vacuum filtration, washed with distilled water and dried at 80 C° overnight.The synthetic zeolite was identified and characterize by the next measurements .From the previous methods its noted that the crystallization of analcime not affected by the hydrothermal reaction time as shown in table 3.Also the synthetic zeolite (analcime) had the same X-ray diffraction this indicate the previous note as shown in figure 2.

**Table (3).** Synthesis conditions and crystallinity data of synthesized analcime.

Sample name	Type of clay	Natural materials	Synthesis time (days)	Synthesis temperature (K)
Analcime -1	kaoline	-	5	443
Analcime -2	Kaoline	-	3	443
Analcime -3	kaoline	Sand	1.5	443

### 3.2. Characterization of synthetic analcime

The various characteristics of the resulting analcime include: X-ray diffraction, scanning electron microscopy, Fourier Transform Infrared (FT-IR) spectroscopy and thermal gravimetric analysis.

#### 3.2.1. X-Ray Diffraction.

The identification and characterizations of the raw material and synthetic zeolite shown in fig.(2). a 2θ range of 5-55°.Kaoline is the predominant mineral phase in the raw material which can be identified by its characteristic XRD peaks at 12.34° and 24.64° 2θ Fig.(2a). However, minor mineral impurities, such as quartz, illite, muscovite and halloysite, also occur. The X-ray diffractograms of the synthesized give reflection peaks at 15.76°, 25.93° and 30.48°As shown in the XRD patterns figure 2b, which is consistent with the analcime [19-20].

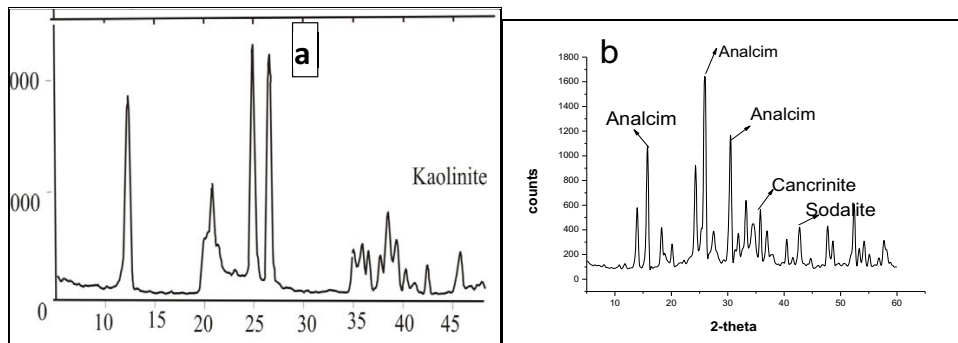


**Figure 2.** XRD patterns of a) Raw material kaolinite b) Synthetic analcime

### 3.2.2. Scanning Electron Microscope (SEM).

The morphology of the raw material and synthetic zeolite were examined as shown in figure 3a, b. The main morphological features observed in the synthesized analcime from met kaolinite are, spherical and cubical.

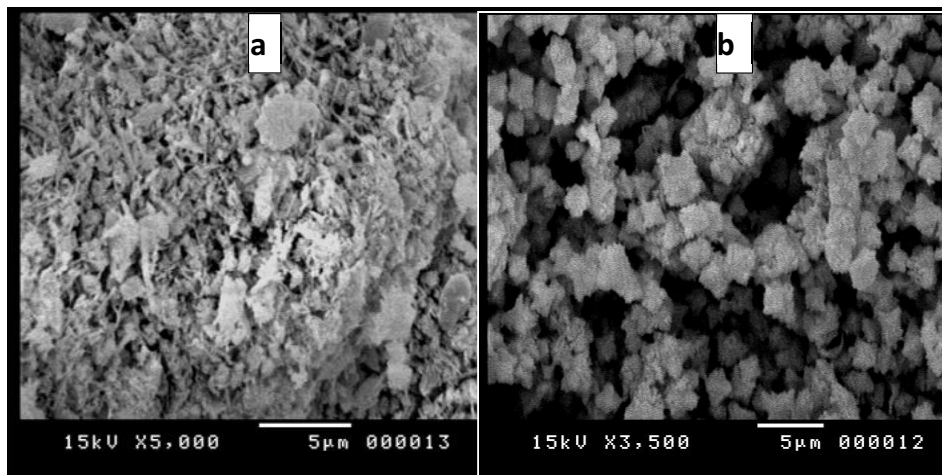


**Figure 3.** SEM micrographs of (a) Raw material kaolinite ;(b) Synthetic analcime

### 3.2.3. Fourier Transform Infrared (FT-IR) Spectroscopy.

The characterization of raw material (kaolinite) and synthetic analcime with transmission Fourier transform infrared spectroscopy (FT-IR) is described in table 4 and figure 4 a, b. The characteristic OH-stretching vibrations of kaolinite band at  $3460.71\text{ cm}^{-1}$ . The symmetric stretch ( $753-71\text{ cm}^{-1}$ ), double ring vibration ( $63-44\text{ cm}^{-1}$ ), T-O bending modes ( $44.04\text{ cm}^{-1}$ ), or the internal linkage vibrations of TO4 (T=Si or Al) tetrahedral and to symmetrical stretching respectively. The bands at ( $1677.26\text{ cm}^{-1}$ ) is assigned to the water in the channels of kaoline. FT-IR spectroscopy is used to probe the structure of the synthesized Analcime and monitor reactions in zeolite pores. Specifically, structural information can be obtained from the vibrational frequencies of the zeolite lattice observed in the range between  $200$  and  $1500\text{ cm}^{-1}$ , (21). In general, each zeolite has characteristic infrared pattern. However, some common features are observed which, include the asymmetric ( $950 - 1250\text{ cm}^{-1}$ ) and symmetric stretch ( $660 - 770\text{ cm}^{-1}$ ), double ring vibration ( $500 - 650\text{ cm}^{-1}$ ), T-O bending modes ( $420 -$

500  $\text{cm}^{-1}$ ), and possibly opening modes (400 - 420  $\text{cm}^{-1}$ ). The FT-IR-spectral data of the synthesized analcime is presented in figure 4b. The double rings (D4R and D6R) in the framework structures of the zeolitic (500 - 650  $\text{cm}^{-1}$ ), is near to 653 (s)  $\text{cm}^{-1}$ , which is characteristic of Analcime, [18]. The bands at 462 (s)  $\text{cm}^{-1}$  of analcime, is near the absorption bands within the range 420–500  $\text{cm}^{-1}$  which are related to the T–O–T bending of vibration mode (T = Al, Si) respectively. These absorption bands characterizing T–O bending vibrations may shifted to lower frequencies due to decreasing Si/Al ratio in the internal linkage due to the different length of the Al–O and Si–O bands [21–22]. The band 724 (s)  $\text{cm}^{-1}$  of analcime is near from the bands in the range 720–790  $\text{cm}^{-1}$  is associated with symmetric stretching vibration of 4-membered rings. Fig. (4b). this band should be assigned to the 4-membered ring vibrations. Because these rings contain the lowest number of members of all rings occurring in the zeolite structure, therefore the bands due to these rings occur at relatively high wave numbers in the pseudo lattice band range [23]. The band 1650 (w), of analcime, is near the bands at 1647 and 1648  $\text{cm}^{-1}$  (Lewis sites) region is assigned to the zeolitic water in the channels of zeolite [24]. The bands at spectra 3446, 3460 and 3482 are attributed to the asymmetric stretching mode of molecular water coordinated to the edges of the zeolite channels [25–26], and the band 3602  $\text{cm}^{-1}$  of analcime is near the bands that are attributed to the asymmetric stretching mode of molecular water coordinated to the edges of the zeolite channels [25] m [26]. The bands that located at the lowest wave numbers 466 and 377  $\text{cm}^{-1}$ , are corresponding to the characteristic bending vibrations carried out in the 4-membered rings. table (4), [27].

**Table 4.** Fourier Transform Infrared (FT-IR) Spectroscopy of Synthetic analcime

	<b>Characteristic band (<math>\text{cm}^{-1}</math>)</b>	<b>Analysis of bands</b>
<b>Analcime</b>	3602 (b)	O—H stretching
	1650 (w)	Bending H—O—H
	1467 (m)	Na-T stretching
	939 (m)	the asymmetric Al –O stretch of sodalite
	724 (s)	4- or 6-membered double rings
	653 (s)	the symmetric Al –O stretch of sodalite
	462 (s)	Sending vibrations of Si-O and Al– O of the tetrahedral

### 3.2.4. Thermal Gravimetric Analysis (TGA) of the synthesized zeolites

The thermal behavior of synthesized analcime (TGA) and (DTG) are shown in table 5, Figure 5. The synthesized product shows up to four dehydration steps. The position of these DTG peaks and the number of dehydration steps can be attributed to the different compensating cation-water binding energies. As well as to the different energy associated with the diffusion of the desorbed water through the porous structure of the synthesized product. Their weight loss percentages reflect the water loss from the zeolite structure, and the amount of desorbed water is related with the number of compensation cations in the framework of the zeolite [28].



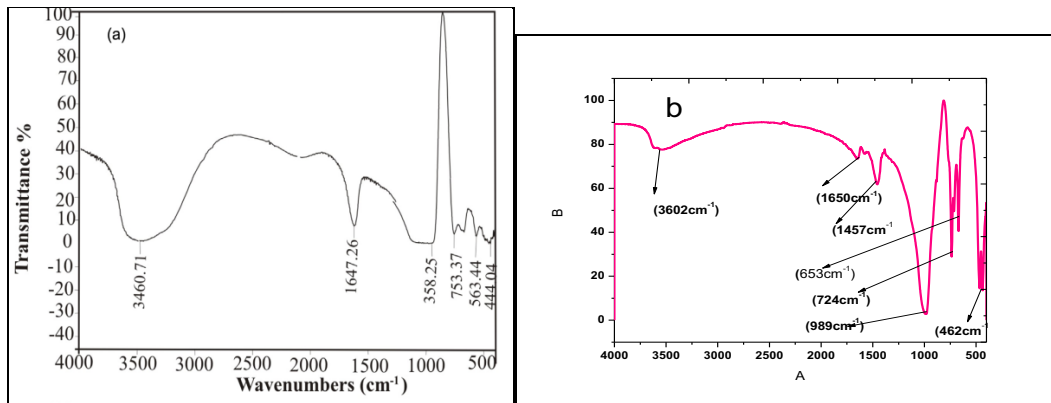


**Figure 4.** Fourier transforms infrared spectroscopy (FT-IR) of (a) Raw material kaolinite, (b) Synthetic analcime

The peaks observed between 39-52 °C correspond to surface water in zeolitic materials; the peaks observed between 100 and 162 °C indicate zeolitic water, although in some cases in this temperature range up to two peaks occur, which can be explained by the heterogeneous nature of the synthesized product. TGA curves also, showed a small weight loss in the range 0-2 % starting at 90°C until 150°C which may be attributed to loss of observed moisture and entrapped solvents. The thermographs of analcime are given in figure 5.

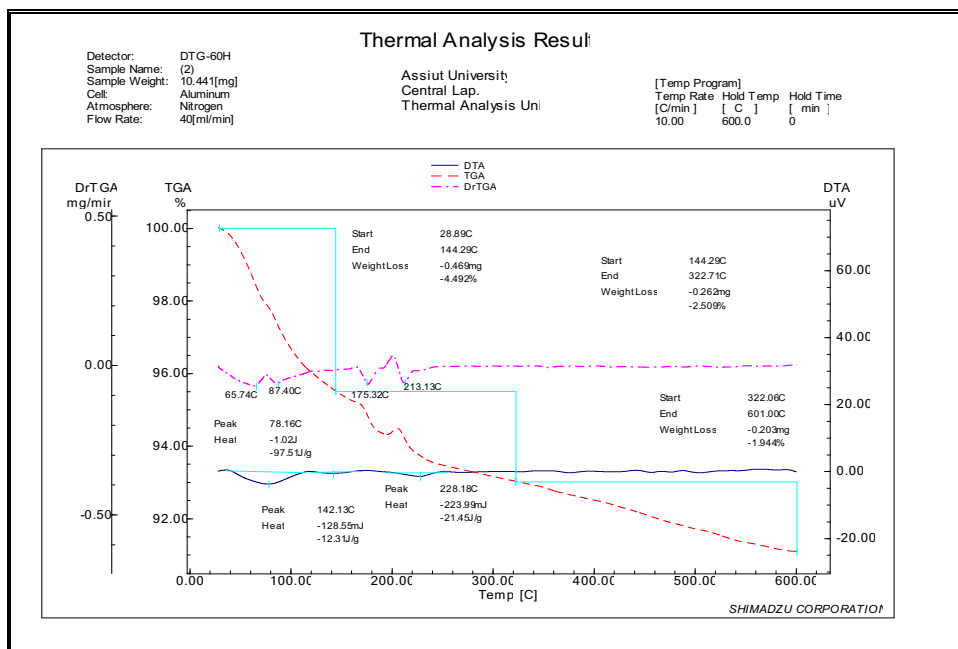


**Figure 5.** Thermal analysis of the synthesized Analcime

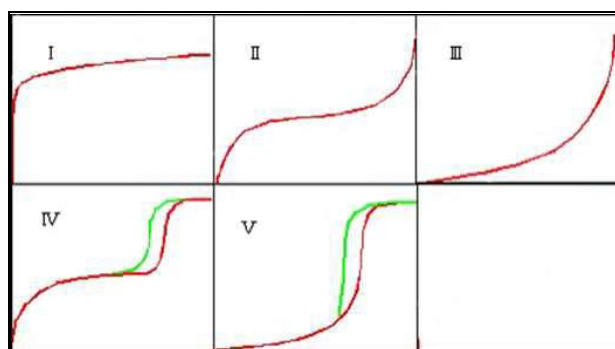
**Table (5):** Thermal analysis of the synthesized zeolites

Type of zeolites	Temperature (°C) for various percentage decompositions *			
	2%	4%	6%	8%
<i>Analcime</i>	85	140	235	470

#### 4. Surface area and porosity of the synthesized Zeolites

##### 4.1. Adsorption Related Properties (Surface Area, Pore Volume, Microspore Surface Area and Pore Size Distribution).

Physical adsorption measurements are widely used to determine the adsorption characteristics such as; surface area, pore volume and pore size distribution. The first step in the presentation of the adsorption isotherm is the identification of the isotherm type and hence the natures of the adsorption process. In this way it is possible to obtain information about the type or pore structure of the adsorbent and this is the most commonly used computational procedure for quantitative evaluation of the isotherm. The physical-sorption isotherms are generally in six forms and presented in figure 6.

**Figure 6.** Types of isotherms

Nitrogen gas adsorption-desorption isotherms were measured at  $-196^{\circ}\text{C}$  using Nova 3200 instrument (Quantachrom Instrument Corporation, USA). Test samples were thoroughly outgassed for 2h at  $250^{\circ}\text{C}$  to a residual pressure of  $10^{-4}$  torr, and the weight of the outgassed sample was that used in calculations. The specific surface area,  $S_{\text{BET}}$  was calculated by applying the BET equation. The porosity of the samples was determined from the desorption curves using Nova enhanced data reduction software, Ver. 2.13. A highly pure nitrogen gas was used as adsorbate. The surface area and porosity of the samples were determined on the basis of nitrogen adsorption and desorption measurement. The measured isotherms exhibit types III isotherms with closed hysteresis loops at intermediate relative pressure. As shown in figure 7. The pore size distribution for these samples could be determined from the desorption data. The specific surface area is derived by applying the BET method in the conventional range of relative pressure with cross-sectional area of  $\text{N}_2 = 16.2 \text{ \AA}^2$ . The values of  $S_{\text{BET}}$ , total pore volume,  $V_{\text{P}}$  (calculated as liquid volume at  $P/P^{\circ} = 0.95$ ), BET-C constant and

the average pore diameter,  $r_H = V_p/S_{BET}$  (parallel plate chap) for each Synthesized Zeolite are given in table 6

**Table 6.** Textural properties of the Synthesized Zeolites

Sample	SBET m <sup>2</sup> /g	C-BET	Total Pore Volume cc/g	Average Pore diameter Å	Exter. Sur. Area m <sup>2</sup> /g	Microp. Sur. Area m <sup>2</sup> /g
<b>Analcime</b>	13.35	-55.79	0.04915	147.235	22.177	0.0000

For mesopores, in view of character of the hysteresis loop, the analysis of the samples showed a single peak distribution that is effectively located at the average pore radius as seen in table 7 indicating a mesoporous structure. BET-C is a constant, which is related exponentially to the heat of adsorption of the first layer. In practice, the value of C can be used to define the measure of heat of adsorption. A high value of C (= 100) is associated with a sharp knee in the isotherm. If C value is low «20 the sharp knee cannot be identified as a single point in the isotherm [29]. The value of C is neither too low nor too high, i.e.  $20 < C < 200$ , and that the BET plot is linear for the P/P<sub>0</sub> region taken for calculations table 9. The value of C may be taken as an indication that basically monolayer-multilayer formation is operative and is not accompanied by any meaningful micro pore filling which is usually associated with an increase in the value C above 200. The pore size analysis is achieved using the corrected model-less method developed for mesopores. In view of character of the hysteresis loop, the analysis of the samples showed a single peak distribution that is effectively located at the average pore radius as seen in table 8, indicating a mesoporous structure. The value of C is neither too low nor too high, i.e.  $20 < C < 200$ , and that the BET plot is linear for the P/P<sub>0</sub> region taken for calculations figure 8. The value of C may be taken as an indication that basically monolayer-multilayer formation is operative and is not accompanied by any meaningful micro pore filling which is usually associated with an increase in the value C above 200 figures 9 and 10.

**Table 7.** Textural properties of the synthesized zeolites

Type of Zeolite	slope	intercept	Correlation coefficient	C-BET	Total surface area in cell m <sup>2</sup>	Specific surface m <sup>2</sup> /g
<b>Analcime</b>	265.47	-4.674426	0.997330	-55.792	1.1083m <sup>2</sup>	13.

**Table 8.** BJHC cumulative pore size distribution (desorption) of the synthesized analcime

Type of Zeolite	Total Pore Volume (cc/g)	Average pore diameters (Å).
<b>Analcime</b>	0.04915	147.238.

**Table 9.** t-method—deBoer (adsorption) of the synthesized analcime

Type of Zeolite	External Surface Area m <sup>2</sup> /g	Microspore Surface Area m <sup>2</sup> /g	Microspore Volume cc/g	Correlation Coefficient
Analcime	22.1765	0.0000	0.00000	0.905983

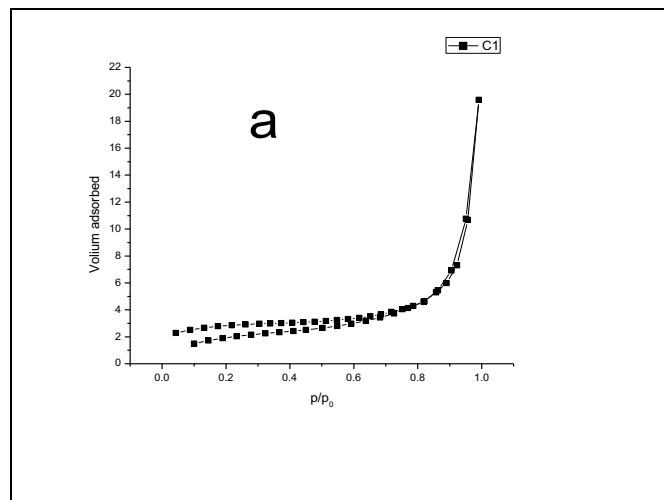


**Figure 7.** Isotherm (Adsorption/Desorption) of analcime

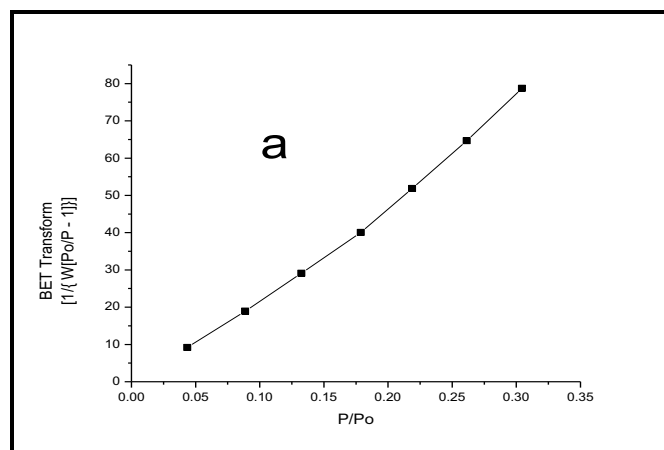


**Figure 8.** Multipoint BET (Adsorption) of Analcime

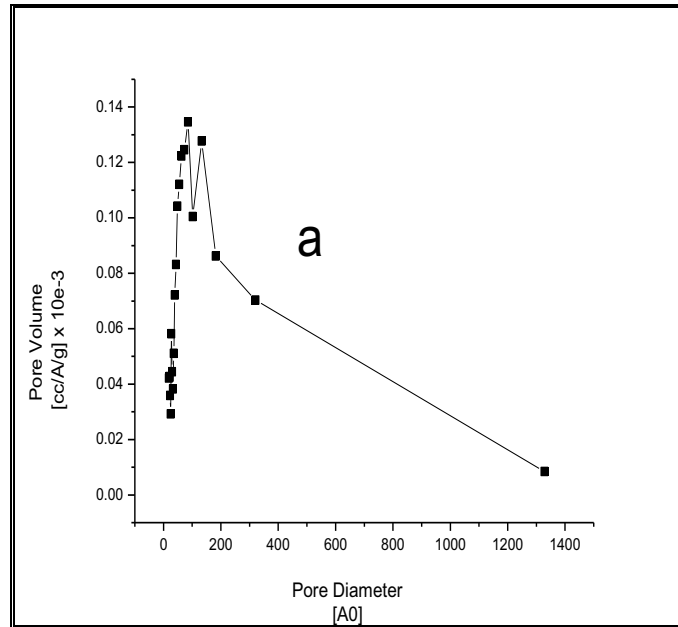


**Figure 9.** BJHdV/Dd (Desorption) of Analcime

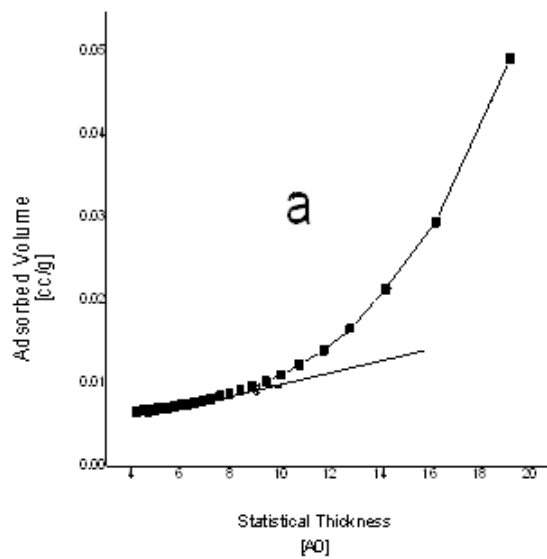


**Figure 10.** tMethod deBoer (Adsorption) of analcime

## 5. Ground water treatment

### 5.1 Nitrate adsorption experiments

The nitrate adsorption experiments were conducted using contaminated ground water samples from Wadi El Assiuti of known initial concentration. Batch experimental mode was adopted due to its simplicity. In the 1st set of experiments,

1- 50 ml of ground water was taken in 100 ml glass beaker.

2- A dose of 0.5 g of synthetic analcime was added

3- The beaker with contents was placed in a thermostatic shaker operated at 200 r/min

4- After 1 h the samples were filtered through a Whatman Filter Paper No. 41.

In a second set of experiments, the effects of adsorbent mass, pH, temperature and time on nitrate removal from water were explored by varying the initial solution pH from (6±0.2) to (10±0.5) and time from 1h to 3h. A final set of experiments involved the use of groundwater samples were analyzed for nitrate levels before contacting them with different doses of sorbents. The equilibrium nitrate concentration was then determined.

## 6. Results and Discussion

### 6.1 Effect of adsorbent mass

The number of active sites relates to adsorbent mass and hence sorption performance. An increase in the solid concentration increases the surface area of the adsorbent, which in turn increases the number of binding sites for the same liquid volume and thus the total amount of metal that is removed increases (30). The effect of adsorbent mass on the nitrate percentage removal under room temperature for 1h and at solution pH is shown in figure 11. It is clear that an increase in adsorbent mass resulted in an increase in the removal of nitrates from water.

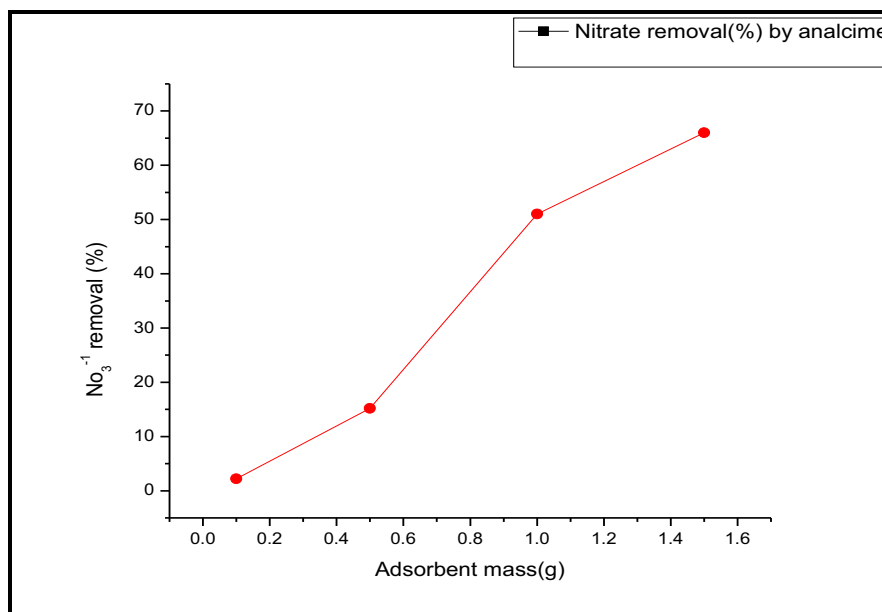


**Figure 11.** Effect of adsorbent mass on nitrate removal from ground water sample by analcime

### 6.2. Effect of pH

Solution pH is one of the factors that have been found to significantly affect the sorption process [31]. A study was therefore undertaken to ascertain to what extent pH affected the sorption of nitrate table 10 is showing initial solution pH (6-8) before and after sorbent addition pH adjustment. The pH was adjusted at equilibrium for system (solution–solid adsorbent). The effect of pH changes on the removal of nitrate have been examined at room temperature, fixed time (1h) and adsorbent (analcime) dosage 0.5g. Results reveal that nitrate removal from ground water is marginally affected by water pH. With no electro kinetic data at this stage, it can only be hypothesized that the surface charge on synthetic (analcime), was significantly affected by pH changes. A confirmation is required to ascertain this. The increasing in nitrate adsorption with decreasing in pH from initial solution pH (6-8) and the highest removal efficiency occurred at pH from (6-6.5). It could be due to interaction during passive transport in the pores and competition between  $\text{OH}^{1-}$  and  $\text{NO}_3^{1-}$  anions for active sites. One disadvantage of using adsorption processes in removal of anionic contaminants from water inheres in most sorption media's inability to perform adequately at higher pH. Indeed several researchers have reported a significant reduction in media performance in nitrate removal from water at near neutral and alkaline pH (6-7.6), the pH range typical of natural systems such as groundwater (32, 33, 34). A media, such as synthetic (analcime) used in this study, whose performance does not deteriorate with pH changes is desirable for water treatment. Meanwhile the pH of the system (solution-solid) after sorption was found to increase when the initial pH was acidic and to decrease when the initial pH was alkaline. This is due to the buffering effect of the zeolite. Sorbents normally shift solution pHs or their point-of-zero charge (pH pzc) [31]. As shown in table 10.

**Table 10.** Effect of pH on Nitrate removal from ground water sample by analcime

Initial pH	Final pH (sol+sorbent)	$\text{NO}_3^{1-}$ Removal (%) by
8	10.4	15
8	9.75	54
6	7.6	78
6	6.5	79
6	6-5.8	58

### 6.3. Effect of temperature

Usually, at elevated temperatures the ions uptake is higher due to higher affinity of the mineral for the metal and/or an increase in the active sites of the solid. At higher temperature the energy of the system facilitates the attachment of ions on the mineral's surface [35]. Analcime can exchange ions at room temperature. When the temperature increases, the ion-exchange occurs more easily. The reason is that there are smaller pores in analcime. The effect of temperature was investigated in a range of 25-45 °C at 1h, dosage 0.5g and solution pH is shown in figure 12 for nitrate adsorption by analcime, it was observed that the decreasing of nitrate concentrations in the water with increasing temperature. Based on that, the nitrate adsorption process is chemical in nature [33], [36]. Consequently, with increasing temperature the retarding specific or electrostatic interactions becomes weaker and the ions become smaller because solvation is reduced. As shown in figure 12.

### 6.4. Effect of time

The effect of contact time on nitrate adsorption from ground water samples using synthetic analcime was given in table 11 and figure 13. Experiments were performed with varying time between 0.25h to 1.5h at normal solution pH (8-8.5), under room temperature and the sorbent mass is 0.5 g per 50 ml water.

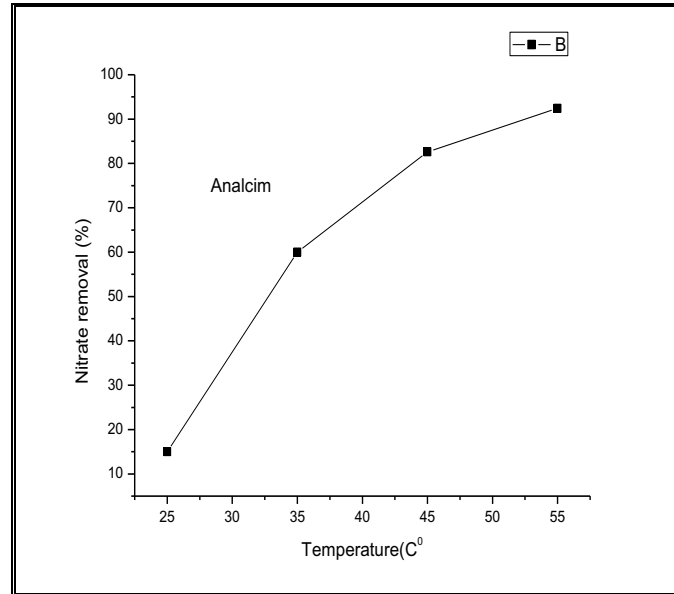


**Figure 12.** Effect of temperature on nitrate removal from ground water sample by analcime

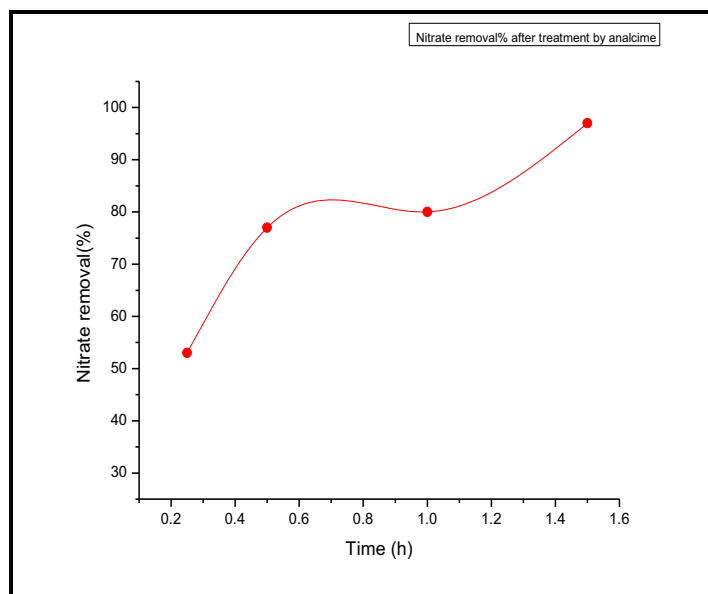


**Figure 13.** Effect of time on nitrate removal from ground water sample by analcime



**Table (11):** Effect of Time on the nitrate removal

$\text{No}_3^{-1}$ conc. (ppm)before treatment	Time (h)	$\text{No}_3^{-1}$ Removal (%) by Analcime
92	1/4	53
	1/2	77
	1	80
	11/2	97

From the results it is clear that with analcime adsorbent the adsorption was rapid in the first 40 min followed by gradual increase with time until equilibrium was attained figure 13. The fast adsorption at the initial stage was probably due to the initial concentration gradient between the adsorbate in the solution and the number of vacant sites available on the adsorbent surface. The attainment of equilibrium adsorption might have been due to reduction in the available active adsorption sites on the adsorbent with time resulting to limited mass transfer of the adsorbate molecules from the bulk liquid to the external surface of adsorbent [37]. So that the ability of both analcime and cancrinite for nitrate removal are affected by time as shown in table 11 and figure 13.

#### 6.5. Mechanism of nitrate removal by analcime

Many studies have been carried out for the removal of nitrate from groundwater for making it potable. However, some of the methods fall short of being reliable and cost effective. Such as Reverse osmosis, Distillation, biological de-nitrification. And adsorption, ion exchange. Adsorption is a phenomenon of adhesion of ions or molecules from one phase into another. Adsorption depends on the surface charge of the media used to adhere the ions called as adsorbent and the charge of ions to be adhered called as adsorbate. Adsorption is most widely researched and still evolving process in water and wastewater treatment. Zeolites have the characteristic of a high adsorption capacity at the lower partial pressure and higher temperature because of the electric field in the cavities and polar actions of zeolites. Also, the zeolite itself is also a kind of polar substance. Also, the water molecules can be bonded to the ions and framework ions by aqueous bridges in the voids of natural zeolites. The water forms bridges between the outer cations. Nitrate is a polyatomic compound of nitrogen with three molecules of oxygen and one molecule of nitrogen bonded by a ligand. Most of the nitrate is in the form of ammonium nitrates or magnesium nitrates which are found in commonly used agricultural fertilizers. The cations in the salts are adsorbed by the clay particles having negative surface charge. This negative charge repulses the anions like nitrate. Thus, the nitrate readily mixes with pore water. For removing nitrate from water, adsorbents with positive surface charge are employed which gives more removal efficiency. Materials with Al and Fe ions are more efficient to remove anion due to their amphoteric nature. They can remove cations and anions depending on the environment like pH, Zeolites are another novel material for removal of impurities and pollutants from water [33]. Analcime (ANA)  $[\text{NaAlSi}_2\text{O}_6 \cdot \text{H}_2\text{O}]$  has the structure and chemical properties similar to the feldspathoids, even though they are classified to the zeolite mineral., classified as such due to its low silicon content. However, cancrinite is classified also as a zeolite, due to its open pore structure, which confers molecular sieve properties [18]. Analcime has a Cubic; tetragonal, orthorhombic, or monoclinic, pseudo cubic, with degree of ordering which can incorporate cations such as  $\text{Na}^+$ ,  $\text{K}^+$  and  $\text{Ca}^{2+}$ , as well

as inorganic anions such as  $\text{CO}_3^{2-}$ ,  $\text{OH}^-$  and  $\text{NO}_3^-$  and water molecules [18]. Analcime can exchange ions at room temperature. When the temperature increases, the ion-exchange occurs more easily. The reason is that there are smaller pores in analcime

#### 6.5.1 Adsorption Isotherm of $\text{NO}_3^-$ ion by synthetic analcime.

Langmuir and Freundlich are the best models to explain the trend of adsorption based on the essence of adsorbents saturated with adsorbate after enough contact time [38-41]. The study were carried out by contacting 0.5g of the previous synthetic zeolites with different concentrations (17,42,74,94 and 100) ppm from solutions under room temperature, for 1 h .and at solution pH on the shaker. The final concentration of nitrate in solution was determined by measuring the absorbance by spectrophotometer (using kits). The data was fitted into the following isotherms: Langmuir, Freundlich, which are shown in tables 12,13,14 and figures 14 a, b.

Langmuir adsorption isotherm is given as equation 1

$$q_e = q_{\max} \times C_e / (K + C_e) \quad (1)$$

Where  $q_e$  is the amount of the solute adsorbed per mass unit of adsorbent (mg/g);  $C_e$  is the equilibrium concentration of the aqueous phase (mg/L); and  $q_{\max}$  is the maximum. Amount adsorbed. The parameters,  $q_{\max}$  and  $K$ , are Langmuir constants. And  $q_e$  can be calculated by equation 2

$$q_e = (C_i - C_e) / X \quad (2)$$

Where  $q_e$  is the amount of the solute adsorbed per mass unit of adsorbent (mg/g),  $C_i$  is the initial concentration in the aqueous phase (mg/L),  $C_e$  is the concentration in the aqueous phase at equilibrium (mg/L),  $V$  is the volume of the aqueous phase (L), and  $X$  is the weight of the adsorbent (g).

Freundlich isotherm is an empirical equation. The nonlinear form of Freundlich's equation is written as equation 3 [42].

$$q_e = K_f C_e^{1/n} \quad (3)$$

Where  $q_e$  is the amount of the solute adsorbed per mass unit of adsorbent (mg/g),  $C_e$  is the equilibrium aqueous pollutant concentration (mg/L),  $K_f$  is Freundlich constant, and  $n$  is Freundlich exponent,  $K_f$  is the indicator of adsorption capacity, and  $1/n$  is a measure of intensity of adsorption. Freundlich is an exponential equation which can be used to determine the values of parameters. The logarithm conversion is one way to determine Freundlich Parameters. Therefore converts to log

$$q_e = \log K_f + 1/n \log C_e$$

By plotting  $\log q_e$  against  $\log C_e$ , the values of Freundlich parameters can be determined. The slope of the line is the exponent and the logarithm of intercept is the constant of Freundlich parameters.

Based on the data given in table 12,13, the plots of  $\log q_e$  versus  $\log C_e$ , and  $1/q_e$  versus  $1/C_e$  were depicted to show the Langmuir and Freundlich isotherms, respectively figures 14 a, b.

The results showed that Langmuir adsorption isotherm had better matching on data with  $R^2 = 0.8$  than Freundlich adsorption isotherm and this confirmed that the sorption data fitted into Langmuir, Freundlich isotherm for sorption of nitrate ion onto the synthetic zeolites (analcime) under the conditions used in the above experiment. Also the characterization of the Langmuir equation can be explained in terms of the equilibrium parameters ( $R_L$ ) which is a dimensionless constant referred to as separation factor or equilibrium parameter equation 4 [43].

$$R_L = 1 / (1 + (K_L + C_0)) \quad (4)$$

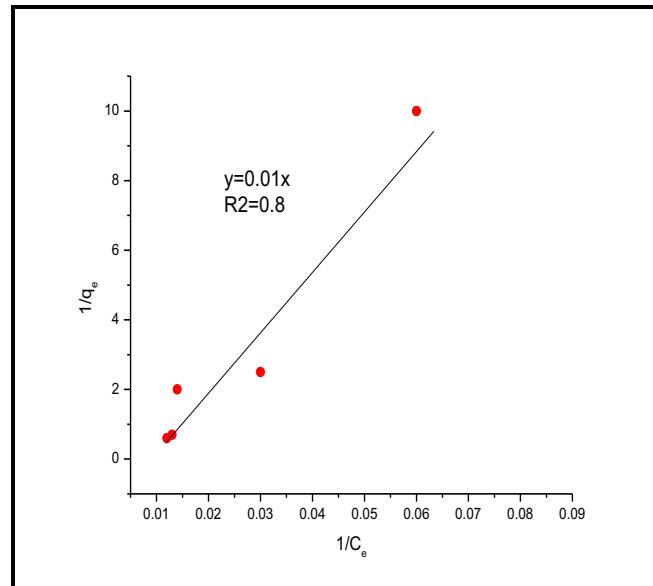


**Figure 14, a.** Langmuir adsorption

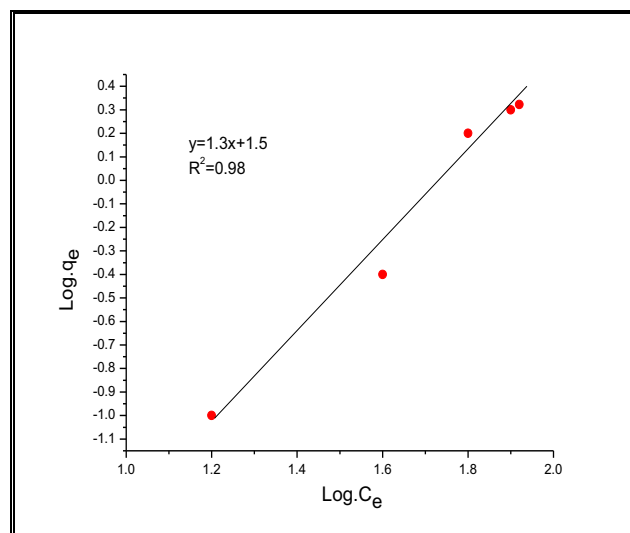


**Figure 14, b.** Freundlich adsorption isotherm

The above parameters describe the nature of the adsorption: irreversible ( $R_L = 0$ ); favorable ( $0 < R_L < 1$ ); linear ( $R_L = 1$ ); unfavorable ( $R_L > 1$ ) [44]. From the data calculated in table (14), in the case of nitrate ion are favorable ( $0 < R_L < 1$ ); And From this research work, the maximum monolayer coverage capacity ( $q_0$ ) from Langmuir Isotherm model was determined to be 0.01 for nitrate ion and  $K_L$  (Langmuir isotherm constant) is 0 for the same ion. This again confirmed that the Langmuir isotherm was favorable for sorption of nitrate ion onto the synthetic zeolite (analcime) under the conditions used in this study [45-46].

**Table 12.** Parameters for plotting Langmuir, Freundlich, and Adsorption Isotherms of nitrate ion by analcime.

$C_0$ (mgNO <sub>3</sub> <sup>-</sup> /L)	$C_e$ (mgNO <sub>3</sub> <sup>-</sup> /L)	$q_e$ (mg/g)	$1/C_e$	$1/q_e$	Log. $C_e$	Log. $q_e$
17	16	0.1	0.06	10	1.2	-1
42	38	0.4	0.03	2.5	1.6	-0.4
74	69	0.5	0.014	2	1.8	0.2
94	76	1.4	0.013	0.7	1.9	0.3
100	80	1.6	0.012	0.6	1.92	0.322

**Table 13.** Linear regress ion equation's Langmuir and Freundlich isotherm and constants for adsorption of nitrate ion by analcime.

Metal ion	Type of zeolites	Langmuir adsorption			Langmuir equations
		$q_m$ (mg/g)	$K_L$ (L/mg)	$R^2$	
NO <sub>3</sub> <sup>-1</sup>	Analcime	0.01	-	0.8	Y=0.01x
		Freundlich adsorption			Freundlich equations
		$1/n$	$n$	$K_F$	
		1.1	0.9	1.5	0.9

**Table 14.**  $R_L$  values for nitrate ion concentrations by analcime

No <sub>3</sub> <sup>-</sup> conc. (ppm) before treatment	17	42	74	94	100
$R_L$ value	0.05	0.023	0.013	0.0099	0.0089

## 7. Conclusions

In this research, analcime was successfully synthesized from cheaper raw materials, such as clay minerals (kaolinite) by using the fusion with NaOH method. The conditions of hydrothermal crystallization (zeolitization) were found to be at temperature of 170°C, and time span between 36 h and 72 h for kaoline. The synthetic materials have been characterized by X-ray diffraction (XRD), scanning electron microscope (SEM), Fourier transform infrared spectroscopy (FT-IR) and thermo gravimetric (DTA/TGA) analysis. Also we used analcime for nitrate removal from groundwater. The first stage of experiments was carried to Batch experimental tests for the ability of analcime for

nitrate removal from for the removal of nitrate ions from the ground water samples from Wadi El-Assiuti – Egypt at initial nitrate concentrations 92 ppm, at solution pH initial pH values (6–8), at time 1h and under normal temperature. It is exhibited the highest nitrate removal efficiency about 79-80% at best pH values of the ground water samples of the studied area (6–6.5), Adsorbent mass 0.5g, at temperature 55 °C for time (1.5h), and initial nitrate concentration of 92mg/L NO<sup>3-</sup>. The Langmuir, Freundlich constants model for NO<sup>3-</sup> ion sorption on the adsorption isotherms are fitted well. The RL value in the present investigation was (0 < RL < 1); indicating that the adsorption of NO<sup>3-</sup> ion by analcime is favorable.

## 8. References

- [1] Magdy H. E., Moustafa M. A. and Hosam A. S. (2012): Impact of hydrochemical Processes on Groundwater Quality, Wadi Feiran, South Sinai, Egypt, Australian Journal of Basic and Applied Sciences, vol.6(3), pp 638-654.
- [2] Apodaca L. E, Jeffrey B. B, Michelle C. S. (2002). Water quality in shallow alluvial aquifers, Upper Colorado River Basin, Colorado, 1997. J. Am. Water Res. Assoc. vol. 38 (1) ,pp.133-143.
- [3] Bhatnagar A., Sillanpää M. . (2011): A review of emerging adsorbents for nitrate removal from water, Chemical Engineering Journal, Volume 168, pp. 493-504.
- [4] Mazeikiene A., Valentukeviciene M., Rimeika M., Matuzevicius AB and Dauknyš R.(2008): Removal of nitrates and ammonium ions from water using sorbent zeolite (clinoptilolite). J. Environ. Eng. Landscape Manage. vol. 16 (1), pp. 38-44.
- [5] Bouwer.H (1989): Agricultural contaminants: Problems and solutions. Water Environ. Technol. vol.1, pp. 292-297.
- [6] Samatya S., Kabay N., Yuksel Ü., Arda M . and Yuüksel. (2006): Removal of nitrate from aqueous solution by nitrate selective ion exchange resins. Reactive Functional Polym. 66 (11) 1206-1214.
- [7] US EPA; (2014): Water: Basic Information about Regulated Drinking Water Contaminants: Basic Information about Nitrate in Drinking Water. Available on: <http://water.epa.gov/drink/contaminants/basicinformation/nitrate.cfm>, Accessed 17 June
- [8] World Health Organization (WHO) (2007): Nitrate and nitrite in drinking water, back ground document for development of WHO Guidelines for Drinking water Quality, WHO/SDE/WSH/07.01/16 /Rev/1.
- [9] Tofighy M. A.; Mohammadi T. (2012): Nitrate removal from water using functionalized carbon nanotube sheets, Journal of Hazardous Materials, Vol. 90, pp. 1815-1822.
- [10] Santafé-Moros A.; Gozávez-Zafrilla J. M.; Lora-García J. (2005): Performance of commercial nanofiltration membranes in the removal of nitrate ions, Desalination, Vol. 185, pp. 281-287 .
- [11] Inglezakis V. J., (2005): The concept of “capacity” in zeolite ion-exchange systems, Journal of Colloid and Interface Science vol. 281, pp. 68–79.
- [12] Sakaalauskas, Valentukeviciene.(2003):investigation into the influence of natural powdered zeolite into drinking water treatment at Druskininkai water workIII, Journal of Environmental Engineering and Ladscepe mangmeneII vol.4,pp.169-178.
- [13] Brannvall E.; Mažeikienė, A.; Valentukevičienė, M. (2006): Experimental research on sorption of petroleum products from water by natural clinoptilolite and vermiculite, Geologija 56: 5–12. ISSN 1392–110X.
- [14] Healey A. M., Johnson G.M., Weller M.T. (2000): The synthesis and characterization of JBW-type zeolites. Part A: Sodium/potassium aluminosilicate, Na<sub>2</sub>K [Al<sub>3</sub>Si<sub>3</sub>O<sub>12</sub>].0.5H<sub>2</sub>O. Microporous and Mesoporous Mater. Vol.37, pp.153-163.
- [15] Gatta G .Nestola, Fabrizio B., Tiziana B. (2004) : Elastic behavior, phase transition, and pressure induced structural evolution of analcime, journal American Mineralogist, vol.91(4),pp. 568-578.

- [16] Fabbrizio, Alessandro S., Max W G., Detlef E., Jost.(2008): Experimental determination of radium partitioning between leucite and phonolite melt and  $^{226}\text{Ra}$ -disequilibrium crystallization ages of leucite, *Journal Chemical Geology*, vol. 255(3), pp. 377-387
- [17] Azizi, Seyed N. T., Salma E. (2013): Cu-modified analcime as a catalyst for oxidation of benzyl alcohol: experimental and theoretical. *Journal Micro porous and Mesoporous Materials*, vol. 167, pp. 89-93
- [18] Ríos C. A., Williams C. D. and Fullen M. A. (2009): Nucleation and Growth History of Zeolite LTA Synthesized from Kaolinite by Two Different Methods. *Applied Clay Science*, vol.42, pp.446-454. <http://dx.doi.org/10.1016/j.clay.2008.05.006>.
- [19] Treacy MMJ, Higgins JB. (2001): Collection of simulated XRD powder patterns for zeolites. Published on behalf of the Structure Commission of the 'International Zeolite Association', *Journal Powder Patterns*, vol.203, pp. 204
- [20] Zhao H, Deng Y, Harsh J B., Flury M., and Boyle J. S. (2004) :Alteration of kaolinite to Cancrinite and Sodalite by Simulated Hanford Tank Waste and its impact on Cesium retention. *claysandclayminerals*, vol.52, pp.1-13.
- [21] Li G. H. (2005): FT-IR Studies of Zeolite Materials: Characterization and Environmental Applications. Ph.D. Thesis, Graduate College, the University of Iowa, Iowa City, 162.
- [22] Mohammed A. A, Shakir I., K. and Esgair K. K. (2013): The Use of Prepared Zeolite Y from Iraqi Kaolin for Fluid Catalytic Cracking of Vacuum Gas Oil. *Journal of Engineering*, vol.19, pp.1256-1270.
- [23] Wang, Haiyan T., Elizabeth A H., Yining. (2006): Investigations of the adsorption of n-pentane in several representative zeolites *Journal of Physical Chemistry B*, vol.110 (16), pp. 8240-8249
- [24] Blanco C., Gonzalez, Pesquera F., Benito C., Mendioroz I. S. and Pajares J.A. (1989) : Differences between One Aluminic Palygorskite and Another Magnesian by Infrared Spectroscopy. *Spectroscopy Letters*, vol. 22, pp.659-673. <http://dx.doi.org/10.1080/00387018908053926>.
- [25] Zhu X.; Choo K.-H.; Park J.-M. (2006): Nitrate removal from contaminated water using polyelectrolyte enhanced ultrafiltration, *Desalination*, Vol. 193, pp. 350-360.
- [26] Faghihian H., and Godazandeha N., (2009): Synthesis of Nano Crystalline Zeolite Y from Bentonite. *Journal of Porous Materials*, vol.16, pp.331-335. <http://dx.doi.org/10.1007/s10934-008-9204-0>
- [27] Mozgawaet W., Jastrzębski W., Handke M. (2005): Vibrational spectra of D4R and D6R structural units. *Journal of Molecular Structure*, vol.744–747, pp.663–670.
- [28] Reyes, Carlos A. R. W., Craig A., Oscar M. C. (2009): Nucleation and growth process of sodalite and cancrinite from kaolinite-rich clay under low-temperature hydrothermal conditions. *Materials Research*, vol.16(2), pp. 424-438.
- [29] Sing, Kenneth SW. (2013): Assessment of surface area by gas adsorption. *J. Adsorption by Powders and Porous Solids: Principles, Methodology and Applications*, pp. 237-263
- [30] Ören, Hakan K.A., Abidin.(2006): Factors affecting adsorption characteristics of  $\text{Zn}^{+2}$  on two natural zeolites, *J. Journal of Hazardous Materials*, vol.131(1-3), pp. 59-65
- [31] Onyango Ms. and Matsuda H. (2006): Fluoride removal from water using adsorption technique. In: Tressaud A (ed.) *Fluoride and Environment: Agrochemical, Archaeology, and Green Chem. And Water (Advances in Fluorine Science, Vol. 2 Elsevier B.V., the Netherlands*. Pp.1-48.
- [32] Chatterjee S., Lee Mw, Lee Ds and Woo Sh. (2009): Nitrate removal from aqueous solutions by cross-linked chitosan beads conditioned with sodium bisulfate. *J. Hazardous Mater.* Vol.166 (1) 508-513.a.
- [33] Chatterjee S. and Woo Sh (2009): The removal of nitrate from aqueous solutions by chitosan hydrogel beads. *J. Hazardous Mater.* Vol.164 (2-3) pp.1012 -1018.
- [34] Cengeloglu, Yunus A., Gulsin T., Ali K., Izzet D., Nesim. (2008): Removal of boron from water by using reverse osmosis. *Separation and Purification Technology*, vol.64 (2), pp. 141-146

- [35] Arief V. O., Trilestari K., Sunarso J., N.Indraswati, Ismadji S. (2008): Recent progress on biosorption of heavy metals from liquids using low cost biosorbents: characterization , biosorption parameters and mechanism studies, *Clean Soil Air Water*, vol.36 ,pp.937–962
- [36] Inglezakis V. J.; Zorpas A. A; Loizidou M. D.; Grigoropoulou, H. P. (2003): Simultaneous removal of metals  $\text{Cu}^{+2}$ ,  $\text{Fe}^{+3}$  and  $\text{Cr}^{+3}$  with anions  $\text{SO}_4^{-2}$  and  $\text{HPO}_4^{-2}$  using clinoptilolite, Microporous and Mesoporous Materials vol.61,pp. 167– 171.
- [37] Sofia M., Sodeh S. , Seyed J.A., and Mohammad O. (2014): Removal of heavy metals from aqueous solution using platinum nanoparticles/Zeolite-4A, *J. Environ Health Sci Eng*, vol.12(7).
- [38] Hamdi W. F, Gamaoun D. E. (2013): Pelster, and M. Seffen, “Nitrate sorption in an agricultural soil profile,” *Applied and Environmental Soil Science*, vol.2013, Article ID 597824, p.7
- [39] Qafoku N. P, Sumner M. E. and Radcliffe D. E. (2000): “Anion transport in columns of variable charge subsoils: nitrate and chloride,” *Journal of Environmental Quality*, vol. 29(2), pp. 484–493,
- [40] Bhatnagar, A. Kumar, E. and Sillanpää, M. (2010): “Nitrate removal From water by nano-alumina: characterization and sorption studies,” *Chemical Engineering Journal*, vol. 163(3), pp. 317– 323
- [41] Hizal J. and Apak R. (2006): “Modeling of cadmium (II) adsorption on kaolinite-based clays in the absence and presence of humic acid,” *Applied Clay Science*, vol. 32, (3-4) pp. 232–244.
- [42] Zheng C. and Bennett G.D. (2002): *Applied Contaminant Transport Modeling*, JohnWiley & Sons, New York, NY, USA, 2nd edition,
- [43] Pandey P. K., Sharma S. K., Sambhi S. S. (2010): Kinetics and equilibrium study of chromium adsorption on zeoliteNaX, *International Journal of Environmental Science & Technology*, vol.7 (2), pp. 395-404
- [44] Rozada F.; Otero M.; García A. I.; Morán. (2007)“A. Application in fixed-bed systems of adsorbents obtained from sewage sludge and discarded tyres, *Journal Dyes Pigment*, vol. 72,(1), pp.47–56.
- [45] Annul, Nurierso, Mustafa, (2006): Adsorption characteristics of heavy metal ions onto a low cost biopolymeric sorbent from aqueous solutions, *Journal of Hazard Mater*, vol. 136 , (2) , pp. 272-280
- [46] Zhao D., Zhou J. and Liu N. (2006): Preparation and Characterization of Mingguang Palygorskite Supported with Silver and Copper for Antibacterial Behavior. *Applied Clay Science*, vol.33, pp.161-170. <http://dx.doi.org/10.1016/j>.